Sugimura K.	but not α-form of prion protein.				
Honda H, Sasaki K, Minaki H, Masui K, Suzuki SO, Doh-ura K, Iwaki T.	Protease-resistant PrP and PrP oligomers in the brain in human prion diseases after intraventricular pentosan polysulfate infusion.	Neuropathology	32(2)	124-132	2012
Hara, H., Okemoto-Nakamura, Y., Shinkai-Ouchi, F., Hanada, K., Yamakawa, Y., and Hagiwara, K.	Mouse prion protein (PrP) segment 100 to 104 regulates conversion of PrPC to PrPSc in prion-infected neuroblastoma cells.	J. Virol.	86	5626-5636	2012
※Okada, H., Iwamaru, Y., Kakizaki, M., Masujin, K., Imamura, M., Fukuda, S., Matsuura, Y., Shimizu, Y., Kasai, K., Mohri, S. and Yokoyama, T.	Properties of L-type bovine spongiform encephalopathy in intraspecies passages.	Vet. Pathol.	49(5)	819-823	2012
Murayama, Y., Imamura, M., Masujin, K., Shimozaki, N., Yoshioka, M., Mohri, S. and Yokoyama, T.	Ultrasensitive detection of scrapie prion protein derived from ARQ and AHQ homozygote sheep by interspecies in vitro amplification.	Microbiol. Immunol.	56(8)	541-547	2012
Okada, H., Murayama, Y., Shimozaki, N., Yoshioka, M., Masujin, K., Imamura, M., Iwamaru, Y., Matsuura, Y., Miyazawa, K., Fukuda, S., Yokoyama, T. and Mohri, S.	Prion in saliva of bovine spongiform encephalopathy–infected cattle.	Emerg. Infect. Dis.	18(12)	2091-2092	2012
Iwamaru, Y., Takenouchi, T., Murayama, Y., Okada, H., Imamura, M., Shimizu, Y., Hashimoto, M., Mohri, S., Yokoyama, T. and Kitani, H.	Anti-prion activity of brilliant blue G.	PLoS One	7(5)	e37896	2012
Dorj G, Okada H, Miyazawa K, Masujin K, Kimura K, Mohri S, and Yokoyama T.	Retrospective analysis of sheep scrapie by western blotting with formalin-fixed paraffin-embedded (FFPE) tissues.	J. Vet. Med. Sci.	74(9)	1207-10	2012
Kim HJ, Tark DS, Lee YH, Kim MJ, Lee WY,	Establishment of a cell line persistently infected with	J. Vet. Med. Sci.	74(10)	1377-80	2012

Cho IS, Sohn HJ, and Yokoyama T.	chronic wasting disease prions.				
Tang Y, Gielbert A, Jacobs JG, Baron T, Andreoletti O, Yokoyama T, Langeveld JP, and Sauer MJ.	All major prion types recognised by a multiplex immunofluorometric assay for disease screening and confirmation in sheep.	J. Immunol. Methods.	29;380 (1-2)	30-9	2012
Murayama, Y., Imamura, M., Masujin, K., Shimozaki, N., Yoshioka, M., Mohri, S. and Yokoyama, T.	Ultrasensitive detection of scrapie prion protein derived from ARQ and AHQ homozygote sheep by interspecies in vitro amplification.	Microbiol. Immunol.	56(8)	541-547	2012
Hasegawa K, Mohri S, and Yokoyama T.	Comparison of the local structural stabilities of mammalian prion protein (PrP) by fragment molecular orbital calculations.	Prion	7(2)	1-7	2013
Iwasaki Y, Yokoi F, Tatsumi S, Mimuro M, Iwai K, Kitamoto T, Yoshida M	An autopsied case of Creutzfeldt-Jakob disease with mutation in the prion protein gene codon 232 and type 1+2 prion protein	Neuropathology	33(5)	568-575	2013
山崎剛士、堀内基広	プリオンの感染と細胞内動態	Dimentia Japan	27	215-224	2013
Sano K., Satoh K., Atarashi R., Takashima H., Iwasaki Y., Yoshida M., Sanjo N., Murai H., Mizusawa H., Schmitz M., Zerr I., Kim YS. and Nishida N.	Early detection of abnormal prion protein in genetic human prion diseases now possible using real-time QUIC assay.	PLoS One.	8(1)	e54915	2013
Hagiwara, K. Hara, H., and Hanada, K.	Species-barrier phenomenon in prion transmissibility from a viewpoint of protein science.	J. Biochem.	153	139-145	2013
中村 優子、萩原 健一	BSE 問題におけるリスク管理とその変遷	ファルマシア	49	48-51	2013
Ohsawa N, Song CH, Suzuki A, Furuoka H, Hasebe R, Horiuchi M.	Therapeutic effect of peripheral administration of an anti-prion protein antibody on mice infected with prions.	Microbiol. Immunol.	57	288-297	2013
※Sakai K, Hasebe R, Takahashi Y, Song CH, Suzuki A, Yamasaki T, Horiuchi M.	Absence of CD14 delays progression of prion diseases accompanied by increased microglial activation.	J. Virol.	87	13433-13445	2013
Nakagaki T, Satoh K,	FK506 reduces abnormal	Autophagy	9(9)	1386-1394	2013

Ishibashi D, Fuse T, Sano K, Kamatari YO, Kuwata K, Shigematsu K, Iwamaru Y, Takenouchi T, Kitani H, Nishida N, Atarashi R.	prion protein through the activation of autolysosomal degradation and prolongs survival in prion-infected mice.				
Higuma M, Sanjo N, Satoh K, Shiga Y, Sakai K, Nozaki I, Hamaguchi T, Nakamura Y, Kitamoto T, Shirabe S, Murayama S, Yamada M, Tateishi J, Mizusawa H	Relationships between Clinicopathological Features and Cerebrospinal Fluid Biomarkers in Japanese Patients with Genetic Prion Diseases	PLoS One	8(3)	e60003	2013
Xiao X, Yuan J, Haïk S, Cali I, Zhan Y, Moudjou M, Li B, Laplanche JL, Laude H, Langeveld J, Gambetti P, Kitamoto T, Kong Q, Brandel JP, Cobb BA, Petersen RB, Zou WQ	Glycoform-selective prion formation in sporadic and familial forms of prion disease	PLoS One	8(3)	e58786	2013
Matsuura Y, Ishikawa Y, Bo X, Murayama Y, Yokoyama T, Somerville RA, Kitamoto T, Mohri S	Quantitative analysis of wet-heat inactivation in bovine spongiform encephalopathy	Biochem. Biophys. Res. Commun.	432 (1)	86-91	2013
Iwasaki Y, Yokoi F, Tatsumi S, Mimuro M, Iwai K, Kitamoto T, Yoshida M	An autopsied case of Creutzfeldt-Jakob disease with mutation in the prion protein gene codon 232 and type 1+2 prion protein	Neuropathology	33(5)	568-75	2013
Takeuchi A, Kobayashi A, Ironside JW, Mohri S, Kitamoto T	Characterization of variant Creutzfeldt-Jakob disease prions in prion protein-humanized mice carrying distinct codon 129 genotypes	J. Biol. Chem.	288 (30)	21659-66	2013
Kobayashi A, Iwasaki Y, Otsuka H, Yamada M, Yoshida M, Matsuura Y, Mohri S, Kitamoto T	Deciphering the pathogenesis of sporadic Creutzfeldt-Jakob disease with codon 129 M/V and type 2 abnormal prion protein	Acta Neuropathol. Commun.	1(1)	74	2013
Iwasaki Y, Tatsumi S, Mimuro M, Mori K, Ito M, Kitamoto T, Yoshida M	Panencephalopathic-type sporadic Creutzfeldt-Jakob disease with circumscribed spongy foci	Clin. Neuropathol.		Epub ahead of print	2013
Sakai K, Hamaguchi T,	Graft-related disease	BMJ Open	23;	e003400	2013

Noguchi-Shinohara M, Nozaki I, Takumi I, Sanjo N, Nakamura Y, Kitamoto T, Saito N, Mizusawa H, Yamada M	progression in dura mater graft-associated Creutzfeldt-Jakob disease: a cross-sectional study		3(8)		
Taguchi Y, Mistica AM, Kitamoto T, Schätzl HM	Critical significance of the region between Helix 1 and 2 for efficient dominant-negative inhibition by conversion-incompetent prion protein	PLoS Pathog	9(6)	e1003466	2013
Hamaguchi T, Sakai K, Noguchi-Shinohara M, Nozaki I, Takumi I, Sanjo N, Sadakane A, Nakamura Y, **Kitamoto T**, Saito N, Mizusawa H, Yamada M	Insight into the frequent occurrence of dura mater graft-associated Creutzfeldt-Jakob disease in Japan	J. Neurol. Neurosurg. Psychiatry	84 (10)	1171-5	2013
Uchiyama K, Miyata H, Sakaguchi S.	Disturbed vesicular trafficking of membrane proteins in prion disease.	Prion	7		2013
Kimura T, Sako T, Siqin, Hosokawa-Muto J, Cui YL, Wada Y, Kataoka Y, Doi H, Sakaguchi S, Suzuki M, Watanabe Y, Kuwata K.	Synthesis of an (11) C-labeled antiprion GN8 derivative and evaluation of its brain uptake by positron emission tomography.	ChemMedChem	8	1035-1039	2013
※ Uchiyama K, Muramatsu N, Yano M, Usui T, Miyata H, Sakaguchi S.	Prions disturb post-Golgi trafficking of membrane proteins.	Nature Commun.	4	1846	2013
Kishimoto Y, Hirono M, Atarashi R, Sakaguchi S,Yoshioka T, Katamine S, Kirino Y.	Age-dependent impairment of eyeblink conditioning in prion protein-deficient mice.	PLoS ONE	8	e60627	2013
Teruya K, Doh-ura K.	Amyloid-Binding Compounds and their Anti-Prion Potency.	Curr. Top. Med. Chem.	13 (19)	2522-2532	2013
倉橋洋史、堂浦克美	プリオン病の診断と治療 プリオン病治療の現状と展望	Clinical Neuroscience	31 (9)	1093-1095	2013
Matsuura, Y., Ishikawa, Y., Somerville, R.A., Yokoyama, T., Hagiwara, K., Yamakawa, Y., Sata, T., Kitamoto, T. and	A rapid bioassay for classical and L-type bovine spongiform encephalopathies	Open Journal of Veterinary Medicine	3	79-85	2013

Mohri, S.					
Yoshioka, M., Matsuura, Y., Okada, H., Shimozaki, N., Yamamura, T., Murayama,Y., Yokoyama, T. and Mohri, S.	Rapid assessment of bovine spongiform encephalopathy prion inactivation by heat treatment in yellow grease produced in the industrial manufacturing process of meat and bone meals.	BMC Vet. Res.	9	134	2013
Imamura, M., Kato, N., Okada, H., Yoshioka, M., Iwamaru, Y., Shimizu, Y., Mohri, S., Yokoyama, T. and Murayama, Y.	Insect cell-derived cofactors become fully functional after proteinase K and heat treatment for high-fidelity amplification of glycosylphosphatidylinositol-anchored recombinant scrapie and BSE prion proteins.	PLoS One	8(12)	e82538	2013
Masujin K, Kaku-Ushiki Y, Miwa R, Okada H, Shimizu Y, Kasai K, Matsuura Y, Yokoyama T	The N-terminal sequence of prion protein consists an epitope specific to the abnormal isoform of prion protein (PrP^{Sc}).	PLoS One	8	e58013	2013
Kasai K, Iwamaru Y, Masujin K, Imamura M, Mohri S, Yokoyama T	Heterogeneity of the abnormal prion protein (PrP^{Sc}) of the Chandler scrapie strain.	Pathogens	2	92-104	2013
横山　隆	動物のプリオン病　牛海綿状脳症(BSE)	Clinical Neuroscience	31	1029-1031	2013
Yamasaki T, Baron GS, Suzuki A, Hasebe R, Horiuchi M.	Characterization of intracellular dynamics of inoculated PrP-res and newly generated PrPSc during early stage prion infection in Neuro2a cells.	Virology	450-451C	324-335	2014
※Okada, H., Iwamaru, Y., Imamura, M., Masujin, K., Matsuura, Y., Fukuda, S., Kageyama, S., Miyazawa, K., Yoshioka, M., Murayama, Y., Yokoyama, T. and Mohri, S.	The presence of disease-associated prion protein in skeletal muscle of cattle infected with classical bovine spongiform encephalopathy.	J. Vet. Med. Sci.	76(1)	103–107	2014
Barria MA, Balachandran A, Morita M, Kitamoto T, Barron R, Manson J, Knight R, Ironside JW, Head MW	Molecular barriers to zoonotic transmission of prions	Emerg. Infect. Dis.	20(1)	88-97	2014
Nishizawa K, Oguma A, Kawata M, Sakasegawa Y, Teruya	Efficacy and mechanism of a glycoside compound inhibiting abnormal prion	J Virol		in press	2014

K, Doh-ura K.	protein formation in prion-infected cells: implications of interferon and phosphodiesterase 4D interacting protein.				
Shirai T, Saito M, Kobayashi A, Asano M, Hizume M, Ikeda S, Teruya K, Morita M, Kitamoto T	Evaluating prion models on comprehensive mutation data of mouse PrP	Structure		in press	2014
※堀内　基広	BSE の発生とその対策を振り返って	日本獣医師会誌		in press	2014

※以下に掲載した論文等

Prion 5:3, 1-4; July/August/September 2011; © 2011 Landes Bioscience

Real-time quaking-induced conversion

A highly sensitive assay for prion detection

Ryuichiro Atarashi,[1,*] Kazunori Sano,[1,2] Katsuya Satoh[1] and Noriyuki Nishida[1,2]

[1]Department of Molecular Microbiology and Immunology; Graduate School of Biomedical Sciences; [2]Global COE Program; Nagasaki University; Nagasaki, Japan

We recently developed a new in vitro amplification technology, designated "real-time quaking-induced conversion (RT-QUIC)," for detection of the abnormal form of prion protein (PrP^{Sc}) in easily accessible specimens such as cerebrospinal fluid (CSF). After assessment of more than 200 CSF specimens from Japanese and Australian patients, we found no instance of a false positive, and more than 80% accuracy for the correct diagnosis of sporadic Creutzfeldt-Jakob disease (sCJD). Furthermore, the RT-QUIC can be applied to other prion diseases, including scrapie, chronic wasting disease (CWD) and bovine spongiform encephalopathy (BSE), and is able to quantify prion seeding activity when combined with an end-point dilution of samples. These results indicate that the RT-QUIC, with its high sensitivity and specificity, will be of great use as an early, rapid and specific assay for prion diseases.

Key words: RT-QUIC, real-time quaking-induced conversion, prion, CJD, Creutzfeldt-Jakob disease, CSF, cerebrospinal fluid

Submitted: 06/10/11

Accepted: 06/28/11

DOI:

*Correspondence to: Ryuichiro Atarashi; Email: atarashi@nagasaki-u.ac.jp

Diagnosis of Creutzfeldt-Jakob Disease: The Current Situation

Human prion diseases, including Creutzfeldt-Jakob disease (CJD), are incurable neurodegenerative disorders characterized by progressive spongiform changes and the accumulation of abnormal prion protein (PrP^{Sc}) in the central nervous system.[1] The majority of CJD cases (approximately 85%) are sporadic in nature, but the remaining cases comprise genetic and infectious forms. Iatrogenic CJD is the consequence of inadvertent transmission during medical procedures in which sporadic CJD (sCJD)-contaminated tissues or explants (such as dura mater and pituitary hormones) or surgical instruments were used.[2] Variant CJD (vCJD) is primarily a zoonosis that arose from contamination of the human food chain by bovine spongiform encephalopathy (BSE), although secondary transmission of vCJD by blood transfusion has also been reported in reference 3. Hence, by adopting additional infection control measures as appropriate, an early and accurate diagnosis of CJD would help to lessen the possibility of iatrogenic transmission and lead the way to timely therapeutic interventions. However, the definitive ante-mortem confirmation of CJD currently requires the presence of typical neuropathology together with the demonstration of PrP^{Sc} in specimens obtained by biopsy, the practice of which is often precluded both by the invasiveness of the procedure and the risks it poses to medical care staff. Thus, the highly sensitive detection of PrP^{Sc} in accessible body fluids such as cerebrospinal fluid (CSF) and blood can be expected to constitute a most valuable means for the early and specific diagnosis of CJD. However, because the concentration of PrP^{Sc} in these specimens is likely to be very low, one of the most promising approaches would be to develop an efficient amplification of PrP^{Sc} in vitro.[4,5] Indeed, several assays, including protein misfolding cyclic amplification (PMCA),[6,7] the amyloid seeding assay (ASA),[8] and quaking-induced conversion (QUIC),[9,10] have previously been reported to permit the sensitive detection of PrP^{Sc} in animal and human brain specimens. Nonetheless, early attempts at

ultrasensitive PrP^{Sc} detection in accessible body fluids were unsuccessful in human prion diseases. For this reason, we initiated studies aimed at establishing a highly sensitive assay for the detection of prion in human CSF.

Establishment of Real-Time QUIC (RT-QUIC)

In the QUIC assays, soluble recombinant PrP (rPrP-sen) expressed in *E. coli* is used as a substrate to amplify the minute amounts of PrP^{Sc}. Using a dedicated shaker, the reaction is enhanced by vigorous intermittent shaking which induces rPrP-sen to aggregate and form fibrils.[9] One of the advantages in QUIC is that shaking/agitation can be performed more easily and consistently than sonication, which has the problem of varied delivery of vibrational energy to the samples. On the other hand, further improvement in the rapidity and practicality of this method was required in order for it to become useful in the diagnosis of prion diseases, because the initial standard format of QUIC (S-QUIC) required a time-consuming western blot. Thus, we combined QUIC technology with thioflavin T (ThT) fluorescence dye, to monitor amyloid formation, in order to minimize the time necessary for the detection of protease-resistant rPrP fibrils (rPrP-res). We first determined if the shaking of our fluorescence microplate reader could induce PrP^{Sc}-dependent rPrP-res (rPrP-res^{Sc}) formation in a buffer containing 0.05–0.1% SDS, as in the S-QUIC. Human rPrP-sen (rHuPrP-sen) and CJD brain homogenate (BH) were used as a substrate and a seed, respectively, for the QUIC reaction. Unexpectedly, we did not observe rPrP-res^{Sc} formation or an elevation in the ThT fluorescence using our microplate reader (unpublished data). Our explanation for this is that the shaking power of the microplate reader was not strong enough to elicit the QUIC reactions in the presence of SDS. SDS tends to cause fibrils to stack and stabilize rPrP-res polymers as a result. In fact, we observed that fibrils formed in the presence of SDS were much larger and thicker than those formed in its absence. Taken together, sonication in PMCA or vigorous shaking in S-QUIC seems to be required as a means of fragmenting the rPrP-res polymers formed in the presence of SDS.

We then tested whether rPrP-res^{Sc} formation was induced when guanidine-HCl (GdnHCl) was added, because it has been thought that GdnHCl was required for the conversion of PrP-sen to PrP-res in a cell-free system.[11] Somewhat unexpectedly, we observed rPrP-res^{Sc} formation even in the absence of GdnHCl. In contrast, the negative control reactions without seed and in the absence of GdnHCl exhibited a marked delay in spontaneous rPrP-res (rPrP-res^{spon}) formation.[12] For this reason, use of a GdnHCl-free buffer can dramatically reduce the risk of false-positive reactions and enhance the sensitivity of the method.

Shaking/agitation is considered to cause several facilitatory effects on the QUIC reaction. One is that a partial unfolding of a portion of the rPrP-sen is induced by increasing the air-water interface through which a denaturing boundary between the hydrophobic air and hydrophilic water is formed.[13] Next, shaking/agitation enhances the interaction between rPrP-sen and PrP^{Sc}, and the fragmentation of rPrP-res polymers.[14] The energetic barrier of spontaneous fibril formation is likely to be higher than that of seed-dependent fibril formation or elongation, because spontaneous formation initially necessitates nucleation as the rate-limiting step.[15]

Meanwhile, the extent of the partial unfolding of rPrP-sen by shaking alone is assumed to be more heterogeneous than that in the presence of GdnHCl, probably because the air-water interfaces are unequally distributed in the reaction mixture (**Fig. 1**). In contrast, the addition of GdnHCl accelerates the nucleation rate, resulting in an increase in the rate of spontaneous fibril formation. Of note, we observed that there was an inverse correlation between the rate of rPrP-res formation and the concentration of rPrP-sen substrate.[12] It has been reported that the aggregation rate of several other proteins is inversely correlated with the concentration of substrate protein in a denaturant-free buffer with shaking.[16,17] Conversely, previous studies using cell-free conversion[18] and rPrP fibril formation,[19-21] respectively, in the presence of denaturant or at low pH, have shown that the rate of PrP-res formation was directly proportional to the PrP-sen concentration. This seeming contradiction can be explained again by the difference in the denaturation status of PrP-sen under various conditions. We hypothesized that heterogenous denaturation of the substrate protein in a denaturant-free buffer with shaking is a major cause of the inverse correlation (**Fig. 1**).

We examined the effect of pH, and the concentrations of rHuPrP-sen and salt, on QUIC reactions in a GdnHCl-free buffer. We found that the presence of NaCl is essential for rPrP-res formation and the sensitivity of this method was maximal at 500 mM NaCl at pH 7.[12] The requirement for NaCl in the formation of rPrP-res is compatible with previous studies, which have shown that salt is required for cell-free conversion in the absence of GdnHCl[22] and the maintenance of a protease-resistant PrP^{Sc} conformation.[23]

We named this new assay "real-time QUIC (RT-QUIC)" by analogy with real-time PCR. The RT-QUIC enabled us to measure up to 96 replicates at a time, obtain the results immediately, and is potentially safer than S-QUIC or PMCA because the prions are sealed within a 96-well plate throughout the entire procedure.

Application of RT-QUIC to Diagnostic Tests for Human Prion Diseases

CJD has been categorized into six molecular subtypes (MM1, MM2, MV1, MV2, VV1, VV2) on the basis of whether methionine (M) or valine (V) is present at codon 129 of the gene encoding prion protein, combined with the profile of PrP^{Sc} (type 1 or type 2).[24] We evaluated the detection limit of MM1- and MM2-sCJD brain homogenate using RT-QUIC. The minimum amount of PrP^{Sc} in the brains detectable by RT-QUIC was around ~1 fg (10^{-15} g). To determine the applicability of RT-QUIC in the clinical diagnosis of sCJD, we compared the RT-QUIC seeding activity in CSF samples from patients with sCJD and patients without sCJD but with other neurodegenerative diseases such as Alzheimer disease. We decided upon CSF as the specimen because CSF is routinely used in the assessment of many

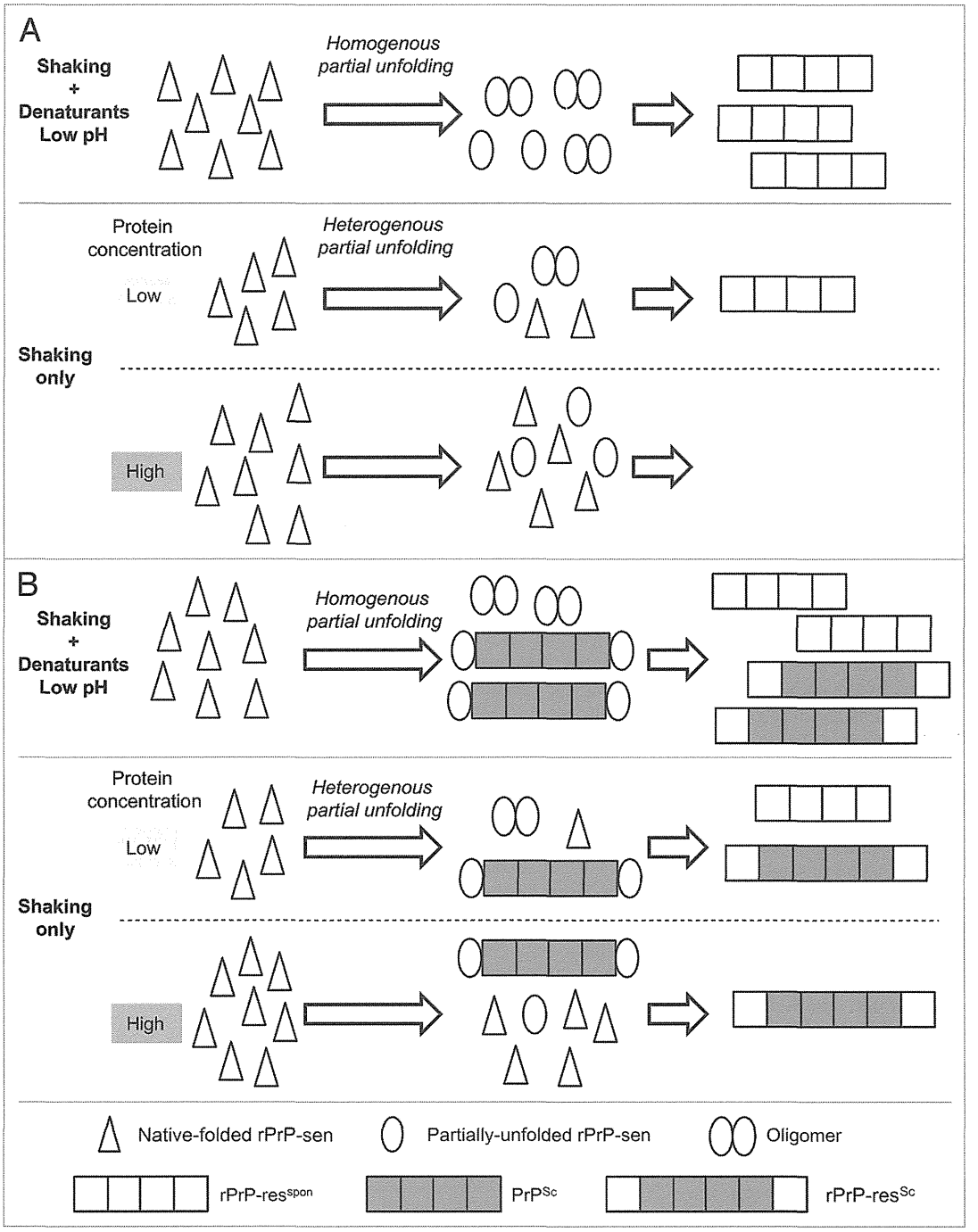

Figure 1. Hypothetical models for the inverse correlation between rPrP-sen concentration and fibril formation in a denaturant-free buffer with shaking in the absence (A) or presence of host-derived PrP^{Sc} (B). Homogeneous partial-unfolding of rPrP-sen is induced in the presence of denaturant or at low pH, leading to an increase of oligomer formation. In contrast, a heterogeneous denaturation status of rPrP-sen is presumed to be inversely proportional to the concentration in a denaturant-free buffer with shaking, resulting in a reduction of oligomer formation. It remains to be determined whether native-folded rPrP-sen can bind to PrP^{Sc} or rPrP-res polymers.

neurological disorders. Moreover, CSF is likely to contain more PrP^{Sc} and fewer impurities than blood. Examining more than 200 CSF specimens from Japanese and Australian patients, we demonstrated that RT-QUIC has greater than 80% sensitivity and absolute specificity for the detection of PrP^{Sc} in the CJD-positive CSF samples.[12] Until now, diagnostic

investigations to evaluate suspected sCJD, although of proven utility, have relied upon non-specific bio-markers, such as the detection of 14-3-3 proteins in the CSF.[25-27] The sensitivity of RT-QUIC was equivalent to and the specificity was much higher than that achieved by 14-3-3 protein measurement. Thus, the RT-QUIC provides a valuable novel means for the antemortem diagnosis of sCJD. Although most of the CSF samples we tested were 129MM, 3/4 129VV and 2/2 129MV CSF samples were positive, suggesting that RT-QUIC using 129M rHuPrP-sen as a substrate is equally valuable in all genetic subtypes of sCJD. Additionally, we recently found that RT-QUIC is potentially useful in the diagnosis of genetic human prion diseases, including Gerstmann-Straussler-Schenker disease (GSS) and fatal familial insomnia (FFI) (manuscript in preparation). While the conversion between PrP-sen and PrP^{Sc} with identical sequences is generally thought to be efficient, our findings suggest that the degree of sequence correspondence between substrate and seed can vary in the RT-QUIC reactions. In support of this concept, we observed that hamster or bovine rPrP-sen can be actively converted into rPrP-res when seeded with sCJD-PrP^{Sc}, albeit with about one log reduction in the detection limit (unpublished data). Furthermore, Orru et al. reported that the use of hamster-sheep chimera rPrP-sen provided for greater sensitivity and less spontaneous fibril formation than was observed with the homologous rHuPrP-sen in the RT-QUIC seeded with vCJD brain homogenate.[28] These results raise the possibility that rPrP-sen may also react to fibrils consisting of other proteins such as beta-amyloid, possibly resulting in a decrease in the specificity of the assay. However, we have yet to experience a single false positive in the RT-QUIC among hundreds of CSF specimens from non-CJD neurodegenerative diseases, including Alzheimer disease, we have tested. Moreover, no increase in ThT fluorescence was observed in the presence of beta-amyloid fibrils artificially formed in vitro (unpublished data). Nevertheless, further studies will be required to completely eliminate the possibility of false positives in the clinical setting. Additionally, the elucidation of the mechanism of rPrP-res^{Sc} formation in the RT-QUIC, including the degree of sequence correspondence, would lead to a better understanding of the molecular basis of prion propagation.

Further Progress in RT-QUIC Technology

Recently, Caughey's group demonstrated that our RT-QUIC could be successfully applied to the detection of hamster and sheep scrapie, deer chronic wasting disease (CWD) and vCJD.[28,29] Additionally, our team has been able to detect BSE at a sensitivity equivalent to that of sCJD (manuscript in preparation). In addition, the RT-QUIC can rapidly determine the relative prion concentration when used in combination with end-point dilution analysis.[29] In another very recent study, Caughey's team showed that enrichment of PrP^{Sc} in plasma by immunoprecipitation employing the PrP aggregate-specific monoclonal IgM antibody 15B3 greatly enhances the sensitivity of RT-QUIC, especially when coupled with a substrate replacement step.[28] Together, these studies demonstrated the wide-ranging application of RT-QUIC to clinical and basic research on human and animal prion diseases.

References

1. Prusiner SB. Prions. Proc Natl Acad Sci USA 1998; 95:13363-83.
2. Hamaguchi T, Noguchi-Shinohara M, Nozaki I, Nakamura Y, Sato T, Kitamoto T, et al. The risk of iatrogenic Creutzfeldt-Jakob disease through medical and surgical procedures. Neuropathology 2009; 29:625-31.
3. Ironside JW. Variant Creutzfeldt-Jakob disease. Haemophilia 5:175-80.
4. Castilla J, Saa P, Morales R, Abid K, Maundrell K, Soto C. Protein misfolding cyclic amplification for diagnosis and prion propagation studies. Methods Enzymol 2006; 412:3-21.
5. Atarashi R. Recent advances in cell-free PrP^{Sc} amplification technique. Protein Pept Lett 2009; 16:256-9.
6. Saa P, Castilla J, Soto C. Presymptomatic detection of prions in blood. Science 2006; 313:92-4.
7. Atarashi R, Moore RA, Sim VL, Hughson AG, Dorward DW, Onwubiko HA, et al. Ultrasensitive detection of scrapie prion protein using seeded conversion of recombinant prion protein. Nat Methods 2007; 4:645-50.
8. Colby DW, Zhang Q, Wang S, Groth D, Legname G, Riesner D, et al. Prion detection by an amyloid seeding assay. Proc Natl Acad Sci USA 2007; 104:20914-9.
9. Atarashi R, Wilham JM, Christensen L, Hughson AG, Moore RA, Johnson LM, et al. Simplified ultrasensitive prion detection by recombinant PrP conversion with shaking. Nat Methods 2008; 5:211-2.
10. Orru CD, Wilham JM, Hughson AG, Raymond LD, McNally KL, Bossers A, et al. Human variant Creutzfeldt-Jakob disease and sheep scrapie PrP(res) detection using seeded conversion of recombinant prion protein. Protein Eng Des Sel 2009; 22:515-21.
11. Kocisko DA, Come JH, Priola SA, Chesebro B, Raymond GJ, Lansbury PT, et al. Cell-free formation of protease-resistant prion protein. Nature 1994; 370:471-4.
12. Atarashi R, Satoh K, Sano K, Fuse T, Yamaguchi N, Ishibashi D, et al. Ultrasensitive human prion detection in cerebrospinal fluid by real-time quaking-induced conversion. Nat Med 2011; 17:175-8.
13. Toth SI, Smith LA, Ahmed SA. Extreme sensitivity of botulinum neurotoxin domains towards mild agitation. J Pharm Sci 2009; 98:3302-11.
14. Collins SR, Douglass A, Vale RD, Weissman JS. Mechanism of prion propagation: amyloid growth occurs by monomer addition. PLoS Biol 2004; 2:321.
15. Lansbury PT Jr, Caughey B. The chemistry of scrapie infection: implications of the 'ice 9' metaphor. Chem Biol 1995; 2:1-5.
16. Sluzky V, Tamada JA, Klibanov AM, Langer R. Kinetics of insulin aggregation in aqueous solutions upon agitation in the presence of hydrophobic surfaces. Proc Natl Acad Sci USA 1991; 88:9377-81.
17. Treuheit MJ, Kosky AA, Brems DN. Inverse relationship of protein concentration and aggregation. Pharm Res 2002; 19:511-6.
18. Caughey B, Kocisko DA, Raymond GJ, Lansbury PT Jr. Aggregates of scrapie-associated prion protein induce the cell-free conversion of protease-sensitive prion protein to the protease-resistant state. Chem Biol 1995; 2:807-17.
19. Baskakov IV, Bocharova OV. In vitro conversion of mammalian prion protein into amyloid fibrils displays unusual features. Biochemistry 2005; 44:2339-48.
20. Jain S, Udgaonkar JB. Evidence for stepwise formation of amyloid fibrils by the mouse prion protein. J Mol Biol 2008; 382:1228-41.
21. Stohr J, Weinmann N, Wille H, Kaimann T, Nagel-Steger L, Birkmann E, et al. Mechanisms of prion protein assembly into amyloid. Proc Natl Acad Sci USA 2008; 105:2409-14.
22. Horiuchi M, Caughey B. Specific binding of normal prion protein to the scrapie form via a localized domain initiates its conversion to the protease-resistant state. EMBO J 1999; 18:3193-203.
23. Nishina K, Jenks S, Supattapone S. Ionic strength and transition metals control PrP^{Sc} protease resistance and conversion-inducing activity. J Biol Chem 2004; 279:40788-94.
24. Parchi P, Giese A, Capellari S, Brown P, Schulz-Schaeffer W, Windl O, et al. Classification of sporadic Creutzfeldt-Jakob disease based on molecular and phenotypic analysis of 300 subjects. Ann Neurol 1999; 46:224-33.
25. Hsich G, Kenney K, Gibbs CJ, Lee KH, Harrington MG. The 14-3-3 brain protein in cerebrospinal fluid as a marker for transmissible spongiform encephalopathies. N Engl J Med 1996; 335:924-30.
26. Zerr I, Bodemer M, Gefeller O, Otto M, Poser S, Wiltfang J, et al. Detection of 14-3-3 protein in the cerebrospinal fluid supports the diagnosis of Creutzfeldt-Jakob disease. Ann Neurol 1998; 43:32-40.
27. Satoh K, Tobiume M, Matsui Y, Mutsukura K, Nishida N, Shiga Y, et al. Establishment of a standard 14-3-3 protein assay of cerebrospinal fluid as a diagnostic tool for Creutzfeldt-Jakob disease. Lab Invest 2010; 90:1637-44.
28. Orru CD, Wilham JM, Raymond LD, Kuhn F, Schroeder B, Raeber AJ, et al. Prion disease blood test using immunoprecipitation and improved quaking-induced conversion. MBio 2011; 2:00078-11.
29. Wilham JM, Orru CD, Bessen RA, Atarashi R, Sano K, Race B, et al. Rapid end-point quantitation of prion seeding activity with sensitivity comparable to bioassays. PLoS Pathog 2011; 6:1001217.

Journal of General Virology (2012), **93**, 668–680 DOI 10.1099/vir.0.037101-0

Characterization of intracellular localization of PrP^{Sc} in prion-infected cells using a mAb that recognizes the region consisting of aa 119–127 of mouse PrP

Takeshi Yamasaki,[1] Akio Suzuki,[1] Takeshi Shimizu,[2] Masahisa Watarai,[3] Rie Hasebe[1] and Motohiro Horiuchi[1]

Correspondence
Motohiro Horiuchi
horiuchi@vetmed.hokudai.ac.jp

[1]Laboratory of Veterinary Hygiene, Graduate School of Veterinary Medicine, Hokkaido University, Kita 18, Nishi 9, Kita-ku, Sapporo 060-0818, Japan

[2]Department of Molecular Infectiology, Graduate School of Medicine, Chiba University, 1-8-1 Inohana, Chiba 260-8670, Japan

[3]Department of Veterinary Public Health, Faculty of Agriculture, Yamaguchi University, 1677-1 Yoshida, Yamaguchi 753-8515, Japan

Received 8 August 2011
Accepted 10 November 2011

Generation of an abnormal isoform of the prion protein (PrP^{Sc}) is a key aspect of the propagation of prions. Elucidation of the intracellular localization of PrP^{Sc} in prion-infected cells facilitates the understanding of the cellular mechanism of prion propagation. However, technical improvement in PrP^{Sc}-specific detection is required for precise analysis. Here, we show that the mAb 132, which recognizes the region adjacent to the most amyloidogenic region of PrP, is useful for PrP^{Sc}-specific detection by immunofluorescence assay in cells pre-treated with guanidine thiocyanate. Extensive analysis of the intracellular localization of PrP^{Sc} in prion-infected cells using mAb 132 revealed the presence of PrP^{Sc} throughout endocytic compartments. In particular, some of the granular PrP^{Sc} signals that were clustered at peri-nuclear regions appeared to be localized in an endocytic recycling compartment through which exogenously loaded transferrin, shiga and cholera toxin B subunits were transported. The granular PrP^{Sc} signals at peri-nuclear regions were dispersed to the peripheral regions including the plasma membrane during incubation at 20 °C, at which temperature transport from the plasma membrane to peri-nuclear regions was impaired. Conversely, dispersed PrP^{Sc} signals appeared to return to peri-nuclear regions within 30 min during subsequent incubation at 37 °C, following which PrP^{Sc} at peri-nuclear regions appeared to redisperse again to peripheral regions over the next 30 min incubation. These results suggest that PrP^{Sc} is dynamically transported along with the membrane trafficking machinery of cells and that at least some PrP^{Sc} circulates between peri-nuclear and peripheral regions including the plasma membrane via an endocytic recycling pathway.

INTRODUCTION

Transmissible spongiform encephalopathies (TSEs) are neurodegenerative disorders characterized by neuronal vacuolization, astrocytosis and accumulation of an abnormal isoform of prion protein (PrP^{Sc}) in the central nervous system. PrP^{Sc} is considered to be a major component of prions, the causative agent of TSE. PrP^{Sc} is a β-sheet-rich structural isomer of a cellular isoform of the prion protein (PrP^{C}) and is generated from PrP^{C} that is encoded by the *Prnp* gene of the host cell (Prusiner, 1998). Infectivity of prions is thought to be associated with PrP^{Sc} oligomers (Silveira *et al.*, 2005); therefore, generation of PrP^{Sc} is a key aspect of prion propagation.

To elucidate the cell biological mechanism of prion propagation, the biosynthesis of PrP^{C} and the generation of PrP^{Sc} have been investigated using cultured cells susceptible to prion infection. A number of biochemical and cell biological analyses have contributed to elucidation of the intracellular dynamics of PrP^{C} (Campana *et al.*, 2005). In contrast to the biosynthesis of PrP^{C}, the mechanisms by which PrP^{Sc} is generated in prion-infected cells are not yet fully understood. One of the obstacles to cell biological analyses of PrP^{Sc} is the difficulty in the specific detection of PrP^{Sc}. Since PrP^{Sc} and PrP^{C} have the same primary structure, most of the antibodies against the PrP molecule cannot distinguish PrP^{Sc} from PrP^{C}. Although some antibodies can specifically immunoprecipitate PrP^{Sc} (Horiuchi *et al.*, 2009; Korth *et al.*, 1997; Paramithiotis *et al.*, 2003), these antibodies are not suitable for the detection of PrP^{Sc} by immunocytochemical analysis. Taraboulos *et al.* (1990) reported that pre-treatment of fixed cells with

guanidinium salts significantly increases the PrP^{Sc} signal following immunofluorescence staining. Although the precise reason as to why PrP^{Sc}-specific detection is achieved by this pre-treatment remains unclear, this method is now used for the PrP^{Sc}-specific detection by immunofluorescence assay (IFA) and immunoelectron microscopy. Earlier studies reported that PrP^{Sc} is mainly localized at the plasma membrane, in secondary lysosomes and at a peri-nuclear Golgi region (Fournier *et al.*, 2000; Jeffrey *et al.*, 1992; McKinley *et al.*, 1991; Taraboulos *et al.*, 1990). However, recent immunocytochemical and immunoelectron microscopy studies showed that PrP^{Sc} is also localized to early endosomes (Veith *et al.*, 2009), late endosomes/multivesicular bodies (Arnold *et al.*, 1995; Pimpinelli *et al.*, 2005) and to endocytic recycling compartment (ERC) at peri-nuclear regions (Godsave *et al.*, 2008; Marijanovic *et al.*, 2009).

In spite of the large contribution of this method on elucidation of the localization of PrP^{Sc} in cells, the specificity

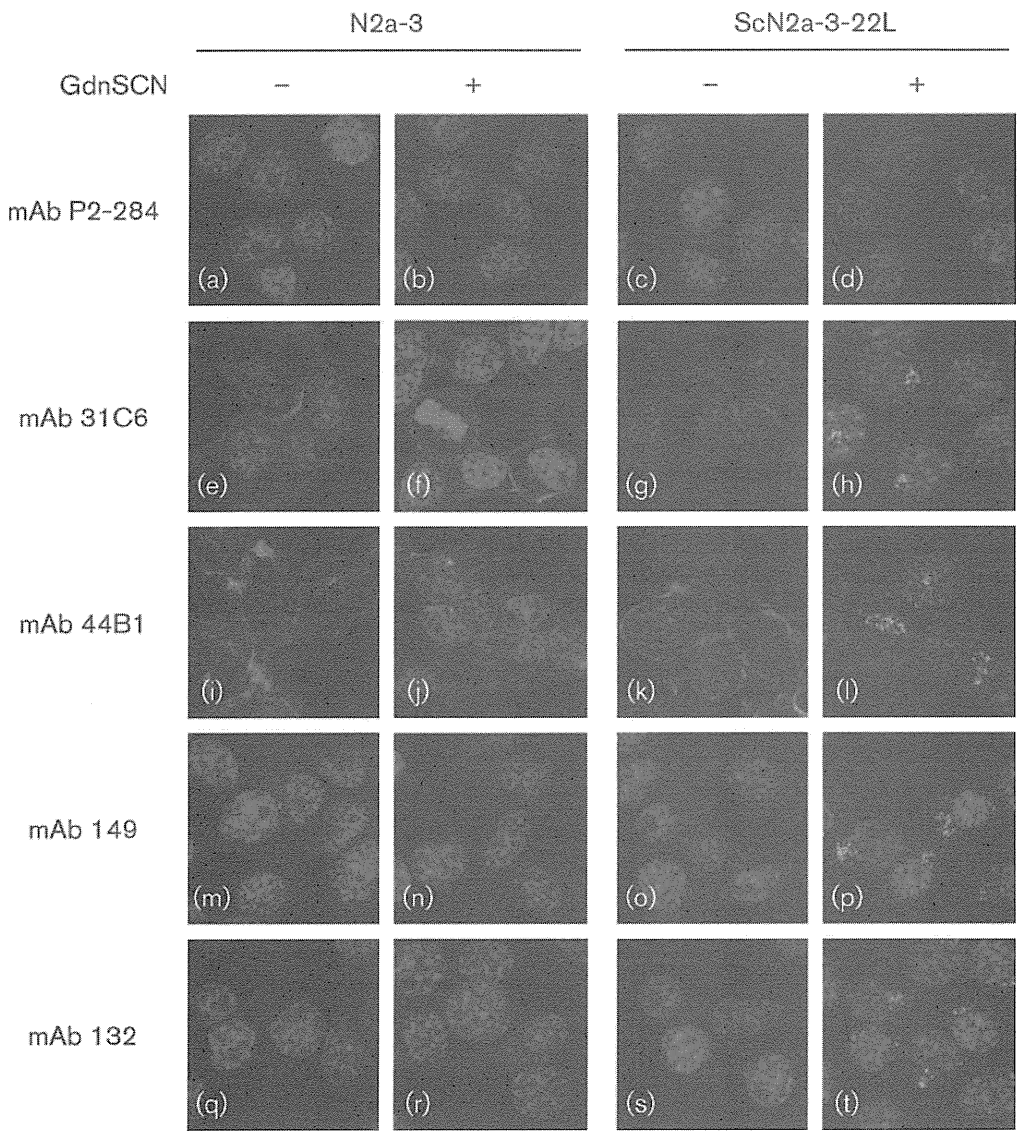

Fig. 1. Reactivity of mAbs to PrP in N2a-3 or ScN2a-3-22L cells with or without GdnSCN pre-treatment in IFA. N2a-3 cells and ScN2a-3-22L cells grown in chamber slides were fixed with 4 % paraformaldehyde and then permeabilized with 0.1 % saponin. The cells were treated with 5 M GdnSCN (b, d, f, h, j, l, n, p, r and t) or were left untreated (a, c, e, g, i, k, m, o, q and s), prior to antibody reaction. The anti-PrP mAbs 31C6 (e–h), 44B1 (i–l), 149 (m–p) and 132 (q–t) were used. The mAb P2-284 was used as a negative control (a–d). Cell nuclei were counterstained with DAPI. Merged images of PrP signals (green) and nuclei (blue) are shown. Nearly 100 % ScN2a-3-22L cells were positive for PrP^{Sc} in IFA using mAb 132.

of PrP^{Sc} detection by this method should be carefully re-evaluated. In fact, pre-treatment with guanidine hydrochloride (GdnHCl) does not prevent detection of PrP^{C} in uninfected cells (Taraboulos *et al.*, 1990; Veith *et al.*, 2009). In order to distinguish PrP^{Sc} from PrP^{C} by IFA, the detector gain or the exposure time needs to be adjusted to a level at which PrP^{C} signals are below the detection limit (Marijanovic *et al.*, 2009; Veith *et al.*, 2009). Alternatively, prior to pre-treatment with denaturants, proteinase K (PK) treatment is required to completely abolish PrP^{C} signals (Taraboulos *et al.*, 1990; Veith *et al.*, 2009). However, PK treatment affects cell architecture, which makes it difficult to finely analyse localization (unpublished observation). Resolution of these technical limitations will improve the quality of PrP^{Sc} detection in prion-infected cells. Taking these background studies into account, we first investigated the utility of various anti-PrP antibodies that recognize different epitopes on the PrP molecule for PrP^{Sc}-specific detection using IFA. We found that the mAb 132, which recognizes linear epitope consisting of mouse PrP aa 119–127 (Kim *et al.*, 2004b), the region adjacent to a hydrophobic amino acid sequence of PrP, AGAAAAGA, was the most suitable for this purpose. We therefore extensively analysed the localization of PrP^{Sc} in prion-infected cells using mAb 132. Our results suggest that PrP^{Sc} is trafficked through a cellular compartment at peri-nuclear regions along with the membrane trafficking machinery of the cells.

RESULTS

Specific detection of PrP^{Sc} in prion-infected cells by IFA

Pre-treatment of cells with denaturants such as guanidinium salts (Taraboulos *et al.*, 1990) and formic acid (Kristiansen *et al.*, 2005) prior to antibody reaction facilitates PrP^{Sc}-specific detection in prion-infected cells by IFA, although the precise mechanism by which this method distinguishes PrP^{Sc} from PrP^{C} remains unclear. However, one concern when using this method is that detection of PrP^{C} cannot be completely excluded as described below. In order to overcome this problem, we evaluated various anti-PrP mAbs for more accurate detection of PrP^{Sc} using IFA.

When N2a-3 cells, a subclone of mouse neuroblastoma Neuro2a cell line (Uryu *et al.*, 2007), without guanidine thiocyanate (GdnSCN) pre-treatment were stained with mAbs 31C6 or 44B1 that react strongly with PrP^{C} expressed on the cell surface, intense PrP^{C} signals were mainly detected at the plasma membrane (Fig. 1e, i). This membrane staining was not affected by GdnSCN pre-treatment (Fig. 1f, j). This result indicates that PrP^{C} was not removed from the cell surface by GdnSCN pre-treatment as described previously (Veith *et al.*, 2009). When N2a-3 cells persistently infected with the prion 22L strain (ScN2a-3-22L) without GdnSCN pre-treatment were stained with these mAbs, PrP signals were also detected at the cell surface similar to N2a-3 cells (Fig. 1g, k). However, staining of ScN2a-3-22L cells that were pre-treated with GdnSCN showed intense granular signals at the peri-nuclear regions (Fig. 1h, l). In addition to this peri-nuclear staining, weak signals at the cell surface were still detected (Fig. 1h, l), especially in areas where the cell density was high (data not shown). The presence of PrP signals at peri-nuclear regions of ScN2a-3-22L cells but not of N2a-3 cells pre-treated with GdnSCN, suggested that these peri-nuclear signals represent PrP^{Sc} as reported previously (Marijanovic *et al.*, 2009; Taraboulos *et al.*, 1990; Veith *et al.*, 2009). However, although signals at the plasma membrane of ScN2a-3-22L cells pre-treated with GdnSCN were much weaker than those of N2a-3 cells, the detection of PrP^{C} in N2a-3 cells after GdnSCN pre-treatment may raise a concern regarding distinction of PrP^{Sc} from PrP^{C}.

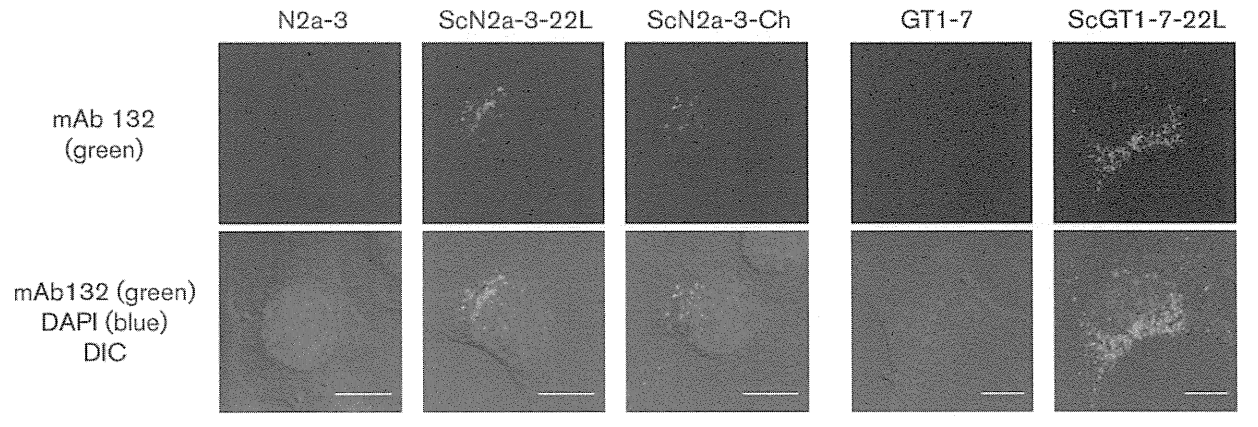

Fig. 2. PrP^{Sc}-specific detection in prion-infected cells using mAb 132. Non-infected N2a-3 and GT1-7 cells as well as ScN2a-3-22L, ScN2a-3-Ch and ScGT1-7-22L cells, were subjected to PrP^{Sc}-specific staining using mAb 132. The images in the upper panel show the PrP^{Sc} signals (green) and those in the bottom panel are differential interference contrast (DIC) images merged with PrP (mAb 132, green) and nuclear (DAPI, blue) fluorescent images. Bars, 10 μm.

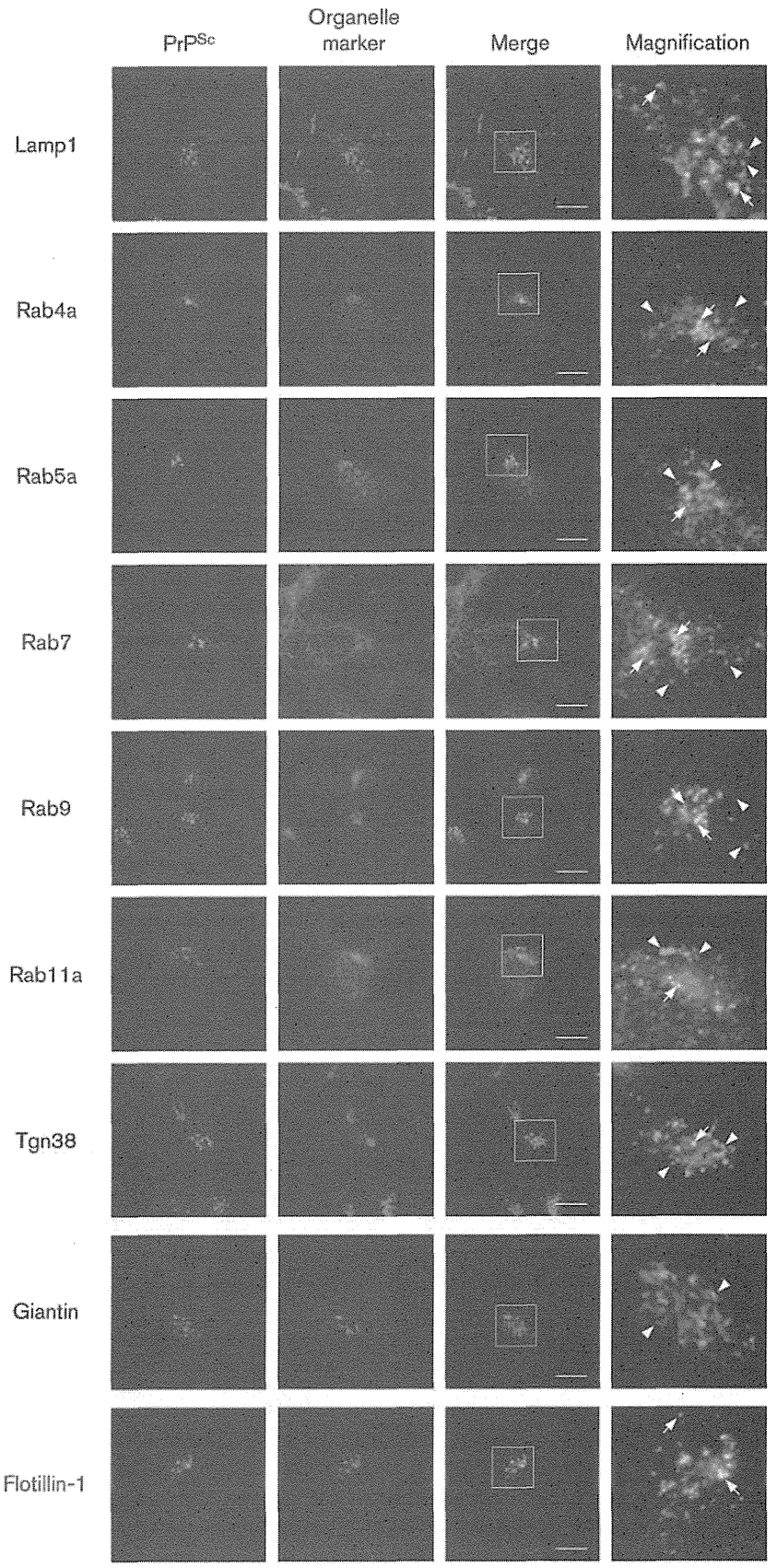

Fig. 3. Intracellular localization of PrP^{Sc}. ScN2a-3-22L cells were stained with the mAb 132 (PrP^{Sc}-specific staining, green) and antibodies against the organelle marker molecules indicated on the left (red). Images in the rightmost column show high magnification images of the boxed regions in the corresponding merged images. The arrows indicate representative examples of co-localization of PrP^{Sc} with the corresponding organelle markers (appear yellow), while the arrowheads indicate PrP^{Sc} that does not co-localize with the corresponding organelle markers (appear green). Bars, 10 μm.

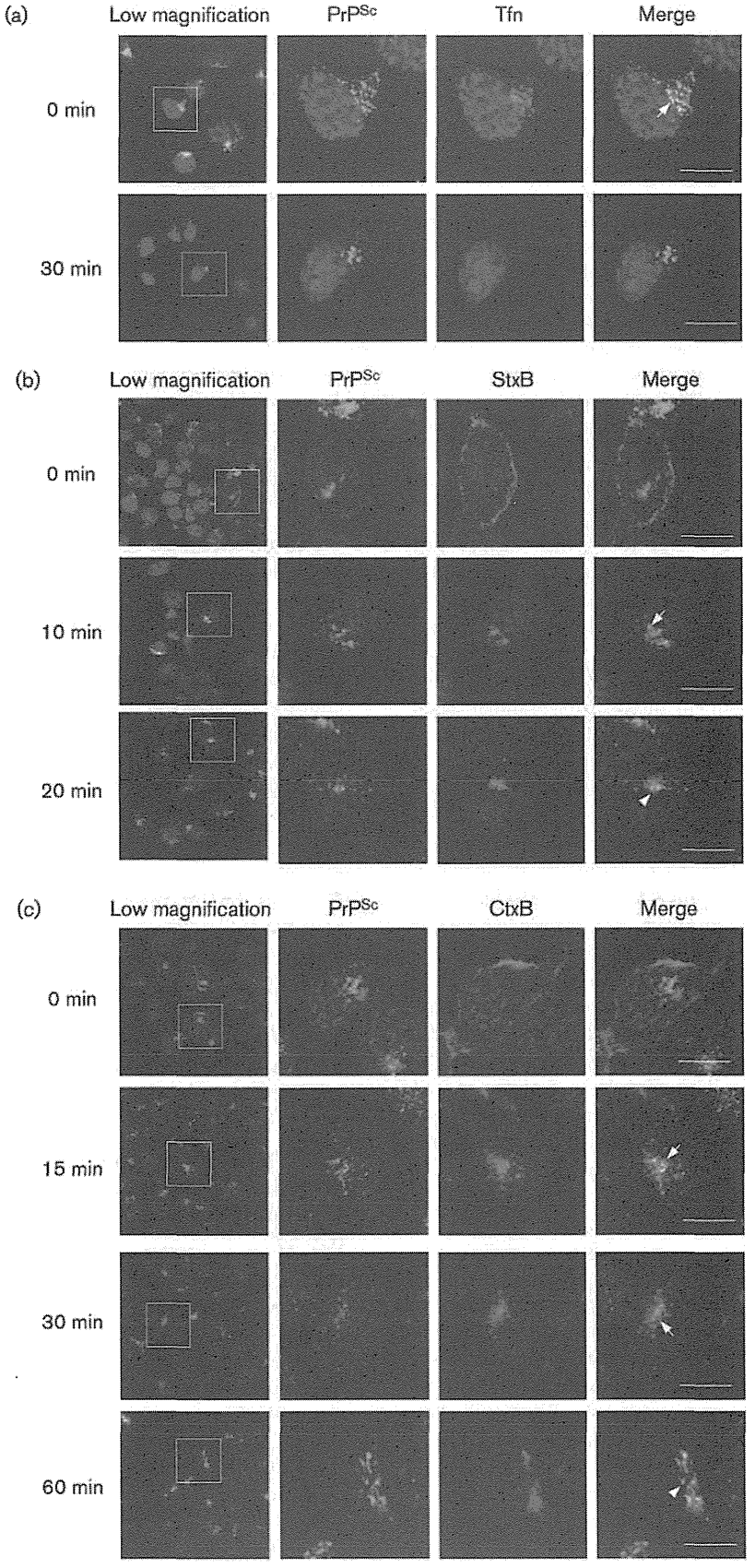
(a)
Low magnification
PrPSc
Tfn
Merge
0 min
30 min
(b)
Low magnification
PrPSc
StxB
Merge
0 min
10 min
20 min
(c)
Low magnification
PrPSc
CtxB
Merge
0 min
15 min
30 min
60 min

Fig. 4. Co-localization of PrP^{Sc} with Tfn, StxB and CtxB. (a) Localization of PrP^{Sc} and Tfn. ScN2a-3-22L cells were incubated with medium containing Alexa-Fluor-555-conjugated Tfn at 37 °C for 15 min (top, 0 min). Subsequently, the cells were cultured with Tfn-free fresh medium at 37 °C for 30 min (bottom, 30 min). All cells were fixed and subjected to PrP^{Sc}-specific staining using the mAb 132. The leftmost column shows a lower magnification of merged images of PrP^{Sc} (green), Tfn (red) and nuclei (blue). Individual and merged high magnification images of the boxed regions are shown on the right. The arrow indicates a representative example of the co-localization of PrP^{Sc} with Tfn. Bars, 10 μm. (b) Localization of PrP^{Sc} and StxB. ScN2a-3-22L cells were incubated with medium containing StxB at 4 °C for 60 min. After incubation, the cells were cultured with StxB-free fresh medium at 37 °C. The cells were fixed at the indicated time points and PrP^{Sc} and StxB were stained using the mAb 132 and anti-StxB rabbit polyclonal antibodies, respectively. The leftmost column shows a lower magnification of a merged image of PrP^{Sc} (green), StxB (red) and nuclei (blue). Individual and merged high magnification images of the boxed regions are shown on the right. The arrow indicates a representative example of co-localization of PrP^{Sc} with StxB, while the arrowhead indicates PrP^{Sc} that is not co-localized with StxB. Bars, 10 μm. (c) Localization of PrP^{Sc} and CtxB. ScN2a-3-22L cells were incubated with medium containing Alexa-Fluor-488-conjugated CtxB at 4 °C for 30 min. After incubation, the cells were cultured with CtxB-free fresh medium at 37 °C. The cells were fixed at each time point and PrP^{Sc} was stained using the mAb 132. The leftmost column shows a lower magnification of a merged image of PrP^{Sc} (green), CtxB (red) and nuclei (blue). Individual and merged high magnification images of the boxed regions are shown on the right. The arrows indicate representative examples of co-localization of PrP^{Sc} with CtxB, while the arrowhead indicates PrP^{Sc} that is not co-localized with CtxB. Bars, 10 μm.

We next tested mAbs 149 and 132, which display little reactivity with PrP^{C} on the surface of N2a cells by flow cytometric analysis (Kim *et al.*, 2004a). mAb 149 detected faint PrP signals in both N2a-3 and ScN2a-3-22L cells without GdnSCN pre-treatment (Fig. 1m, o). However, GdnSCN pre-treatment abolished the faint PrP^{C} signals detected in N2a-3 cells, but enhanced strong granular signals at peri-nuclear regions in ScN2a-3-22L cells (Fig. 1n, p). mAb 132 staining resulted in intense PrP signals at peri-nuclear regions in ScN2a-3-22L cells pre-treated with GdnSCN (Fig. 1t). Remarkably, this mAb detected little PrP^{C} in N2a-3 cells, regardless of the presence or absence of GdnSCN pre-treatment (Fig. 1q, r). Moreover, PrP signals in ScN2a-3-22L cells without GdnSCN pre-treatment appeared to be below the detection limit (Fig. 1s). We also verified the utility of mAb 132 for PrP^{Sc}-specific detection in different prion strains or cell lines (Fig. 2). Similar to ScN2a-3-22L cells, characteristic granular signals were detected in N2a-3 cells infected with the Chandler strain (ScN2a-3-Ch) and in GT1-7 cells persistently infected with the 22L strain (ScGT1-7-22L), but fluorescent PrP^{C} signals in uninfected cells remained at background level. Since hardly any PrP^{C} signal was detected in uninfected cells even after GdnSCN pre-treatment, mAb 132 is believed to enable more precise PrP^{Sc}-specific detection in IFA.

Intracellular localization of PrP^{Sc}

Since mAb 132 enables reliable PrP^{Sc}-specific detection, we used this mAb to analyse the intracellular localization of PrP^{Sc} in ScN2a-3-22L cells. Lamp1, a marker of late endosomes and/or lysosomes, has been reported to co-localize with PrP^{Sc} in prion-infected cells (Pimpinelli *et al.*, 2005). As expected, some PrP^{Sc} did co-localize with Lamp1 at peri-nuclear and peripheral regions of the cell (Fig. 3, arrows). However, PrP^{Sc} that was detected in a region extremely close to the nucleus did not co-localize with Lamp1 (Fig. 3, arrowheads).

We further analysed the co-localization of PrP^{Sc} with Rab GTPases that are known to be present in distinct organelles (Stenmark, 2009; Grant & Donaldson, 2009). Peri-nuclear PrP^{Sc} partially co-localized with Rab4a, a marker of early endosomes including rapid endocytic recycling endosomes; Rab5a, a marker of early endosomes; Rab7, a marker of late endosomes; Rab9, a marker of late endosomes involved in retrograde transport to the *trans*-Golgi network; and Rab11a, a marker of ERC (Fig. 3, arrows). In contrast to the co-localization of PrP^{Sc} with endosomal and lysosomal markers, only a small proportion of PrP^{Sc} co-localized with Tgn38, a marker of the *trans*-Golgi network. However, peri-nuclear PrP^{Sc} did not appear to co-localize with giantin, a marker of the *cis*/medial-Golgi (Fig. 3).

Flotillin-1 is a protein that is associated with lipid rafts and is known to be present at the plasma membrane, the *trans*-Golgi network and in endosomes, lysosomes and lipid droplets (Browman *et al.*, 2007). In contrast to the partial co-localization of PrP^{Sc} with the endosomal and lysosomal markers described above, a large proportion of PrP^{Sc} appeared to co-localize with flotillin-1 (Fig. 3).

PrP^{Sc} is localized to ERC in the intracellular transport pathway of transferrin (Tfn), Shiga toxin B subunit (StxB) and Cholera toxin B subunit (CtxB)

Recent ultrastructural and immunofluorescence studies have revealed that PrP^{Sc} is localized in endocytic compartments (Godsave *et al.*, 2008; Marijanovic *et al.*, 2009; Pimpinelli *et al.*, 2005; Veith *et al.*, 2009). Since PrP^{Sc} is often detected at the peri-nuclear regions very close to but not in the Golgi apparatus, of particular interest is the ERC that is located near the microtubule organizing centre and the Golgi apparatus that is involved in the recycling of membrane lipids and proteins (Grant & Donaldson, 2009). Therefore, to more precisely analyse juxtanuclear PrP^{Sc} localization, we used Tfn as a marker for the ERC. Tfn

binds the Tfn receptor that is internalized from the cell surface via clathrin-coated pits, is transported to early endosomes, and is then recycled back to the plasma membrane via the ERC (Maxfield & McGraw, 2004). When the cells were loaded with Alexa-Fluor-555-conjugated Tfn, Tfn was detected at the peri-nuclear regions 15 min after the initiation of uptake (time 0) and Tfn had almost disappeared 30 min after the removal of Tfn from the medium (Fig. 4a). Some of the juxtanuclear PrP^{Sc} did co-localize with internalized Tfn at peri-nuclear regions 15 min after Tfn loading, suggesting that the ERC is one of the compartments to which PrP^{Sc} localizes.

Flotillin-1 is reported to be involved in clathrin-independent endocytosis of StxB and CtxB (Glebov *et al.*, 2006; Lin & Guttman, 2010). StxB and CtxB are known to bind globotriaosylceramide and GM1 ganglioside, respectively, at cell surface and are transported from the plasma membrane to the *trans*-Golgi network via early endosomes and the ERC (Lieu & Gleeson, 2010; Nichols *et al.*, 2001). Since PrP^{Sc} clearly co-localized with flotillin-1 (Fig. 3), we further analysed the localization of PrP^{Sc} with StxB and CtxB. When cells were loaded with StxB at 4 °C and StxB was then internalized by transfer of the cells to 37 °C, StxB partly co-localized with PrP^{Sc} at the peri-nuclear region 10 min after initiation of internalization (Fig. 4b, arrow). However, co-localization of PrP^{Sc} with StxB was not so clear after further 10 min incubation (Fig. 4b, arrowhead). Similarly, co-localization of PrP^{Sc} with internalized CtxB was observed at the peri-nuclear regions 15 and 30 min after initiation of internalization, but co-localization was weaker after 60 min (Fig. 4c). At 15–30 min after initiation of internalization, CtxB at the peri-nuclear regions showed strong co-localization with Rab11a, but after 60 min, it co-localized more strongly with Tgn38. This result suggested that CtxB present at the peri-nuclear regions was mainly in the ERC at 15–30 min, and in the *trans*-Golgi network at 60 min after initiation of internalization (Fig. 5, 37 °C). These results indicate that PrP^{Sc} is present in the ERC, which is on the intracellular transport pathway of StxB and CtxB.

PrP^{Sc} dynamically cycles between peripheral and peri-nuclear regions in ScN2a-3-22L

The presence of PrP^{Sc} in various endocytic compartments, especially in the ERC through which Tfn, StxB and CtxB are transported, suggested that PrP^{Sc} is transported intracellularly by the membrane trafficking machinery of the cell, rather than being a permanent resident of these organelles. To address the association of PrP^{Sc} with the intracellular membrane trafficking machinery, we analysed the localization of PrP^{Sc} in ScN2a-3-22L cells that were incubated at 20 °C. Incubating cells at a low temperature ($\leqslant$20 °C) impairs the transport of Tfn or StxB from the plasma membrane to peri-nuclear regions (Mallard *et al.*, 1998; Ren *et al.*, 1998; Sipe *et al.*, 1991). We firstly confirmed that incubation of ScN2a-3-22L cells at 20 °C slowed down the transport of CtxB (Fig. 5) and StxB (data not shown). Following incubation at 37 °C, CtxB was concentrated at the peri-nuclear regions and co-localized with Rab11a within 15–30 min and with Tgn38 within 60 min, after initiation of its uptake. In contrast, CtxB did not co-localize with either Rab11a or Tga38 after 30 min of incubation at 20 °C, but co-localization with Rab11a could be observed 60 min after the start of incubation. In addition, some CtxB still remained at the plasma membrane 60 min after the incubation, indicating that the transport of CtxB from the plasma membrane to peri-nuclear regions had been slowed down. Under this condition, most of the PrP^{Sc} signals disappeared from the peri-nuclear regions and appeared at peripheral regions of the cells, including at the plasma membrane, within 1 h (Fig. 6a, 20 °C/1 h, arrowheads). After subsequent incubation for another hour, some of the PrP^{Sc} seemed to have redistributed to the peri-nuclear regions (Fig. 6a, 20 °C/2 h), following which, PrP^{Sc} gradually disappeared again from the peri-nuclear regions over the next 10 h of incubation. Indeed, following this incubation, the majority of PrP^{Sc} redistributed to the peripheral regions of the cells (Fig. 6a, 20 °C/12 h).

When ScN2a-3-22L cells that had been incubated at 20 °C for 12 h were transferred to 37 °C, peri-nuclear PrP^{Sc} signals appeared to increase and PrP^{Sc} signals at the peripheral regions appeared to decrease within 30 min of incubation (Fig. 6a, 37 °C/30 min). Interestingly, after an additional 30 min incubation at 37 °C, some of the PrP^{Sc} reappeared at the peripheral regions including the plasma membrane, although some PrP^{Sc} was still detected at the peri-nuclear regions (Fig. 6a, 37 °C/60 min, arrowheads). During subsequent 1 h incubation, PrP^{Sc} signals at the peripheral regions decreased again, and thereafter, signals of PrP^{Sc} at the peri-nuclear regions appeared to revert to the steady-state level (Fig. 6a, 37 °C/120 min). Little PrP^{C} was detected in N2a-3 cells throughout the experimental period (Fig. 6b), which means that both the peri-nuclear and the peripheral fluorescent signals represent PrP^{Sc}. In spite of the changes in the intracellular distribution of PrP^{Sc}, the amount of PrP-res, a representative of a protease-resistant form of PrP^{Sc}, was unchanged over the experimental period (Fig. 7). These results suggest that the dynamic changes in the distribution of PrP^{Sc} were not due to major differences in synthesis or degradation of PrP^{Sc} at specific regions of the cell, but were primarily due to the intracellular trafficking of PrP^{Sc} through the peri-nuclear regions.

DISCUSSION

Analysis of the intracellular localization of PrP^{Sc} is important for the understanding of the cellular mechanism of prion propagation. Taraboulos *et al.* (1990) showed that pre-treatment of prion-infected cells with GdnHCl enables PrP^{Sc}-specific detection using IFA. Although the mechanism of

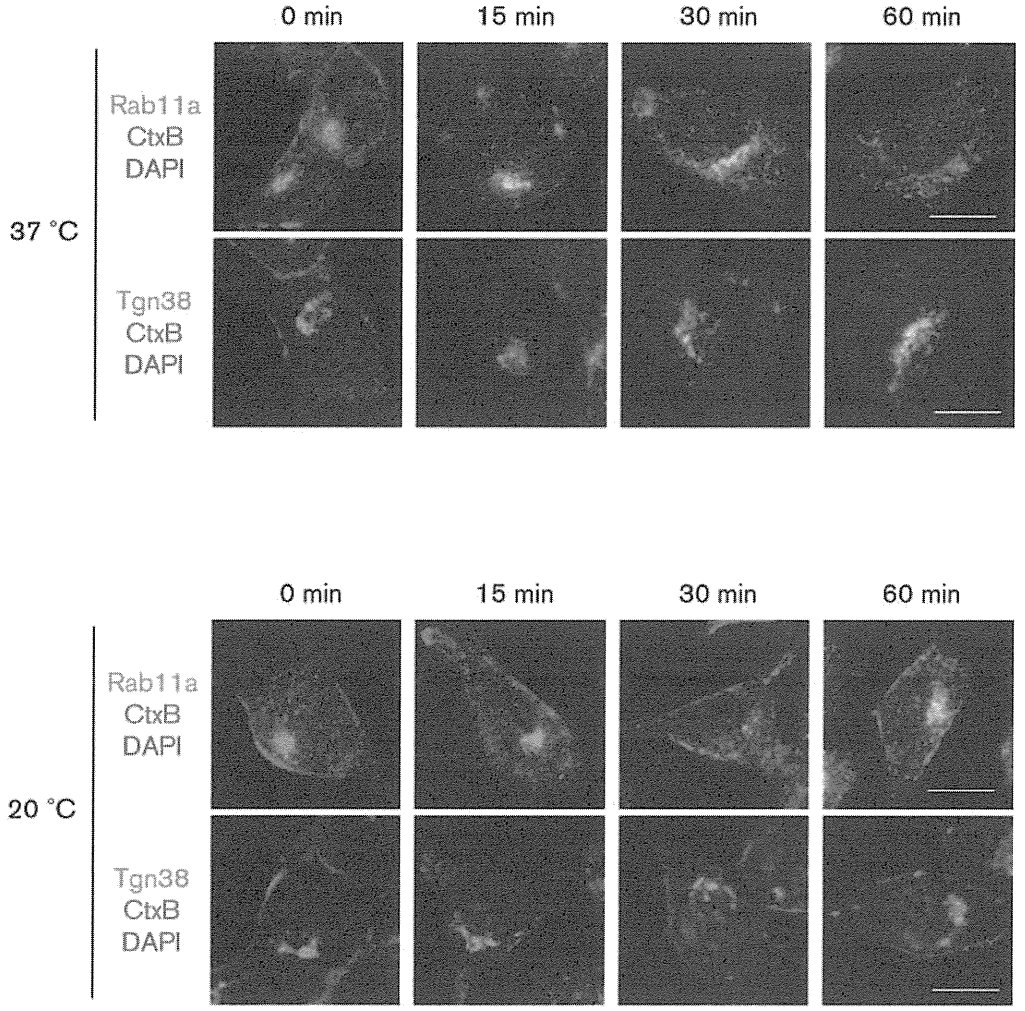

Fig. 5. Localization of CtxB with marker molecules. ScN2a-3-22L cells were incubated with medium containing Alexa-Fluor-488-conjugated CtxB at 4 °C for 30 min and the medium was then replaced with CtxB-free fresh medium. The cells were then incubated at 37 °C (top panel) or 20 °C (bottom panel) for up to 60 min. The cells were fixed at each time point and stained with anti-Rab11a or anti-Tgn38 rabbit polyclonal antibodies. Merged images of Rab11a or Tgn38 (green) with CtxB (red) and nuclei (blue) are shown. Bars, 10 μm

PrP^{Sc}-specific detection by pre-treatment of cells with chaotropic agents was unclear, this method has been used for the detection of PrP^{Sc} in cells and tissues (Marijanovic *et al.*, 2009; Pimpinelli *et al.*, 2005; Taraboulos *et al.*, 1990; Veith *et al.*, 2009). Treatment with denaturant facilitates exposure of cryptic epitopes of PrP^{Sc} (Taraboulos *et al.*, 1990). However, since GdnHCl treatment does not remove PrP^{C} from uninfected cells (Taraboulos *et al.*, 1990; Veith *et al.*, 2009; this study), detection of PrP^{C} signals would be expected because most of the antibodies against PrP molecules react not only with denatured PrP^{Sc} but also with denatured PrP^{C}. If signals from the denatured PrP^{Sc} are strong enough to distinguish them from PrP^{C}, then PrP^{Sc}-specific detection can be achieved by setting the threshold level just above the level of PrP^{C} signals by manipulation of the gain of detector, changing exposure time and so on. However, such adjustment will miss subtle details of the PrP^{Sc} signals. Therefore, further improvement of PrP^{Sc}-specific detection is still required for detailed characterization of the intracellular localization of PrP^{Sc}. To improve the specificity of PrP^{Sc} detection, we used mAb 132, which recognizes the epitope consisting of mouse PrP aa 119–127, adjacent to the hydrophobic amino acid sequence, AGAAAAGA (Gasset *et al.*, 1992). Since mAb 132 showed little reactivity with native PrP^{C} on the cell surface, the epitope for mAb 132 is thought to be buried inside the PrP^{C} molecule. Denaturation with GdnSCN was expected to expose the epitope for mAb 132 of PrP^{C}, but in fact, mAb 132 showed little reactivity with PrP^{C} in uninfected cells even after treatment with GdnSCN (Fig. 1). A reduction in PrP^{C}

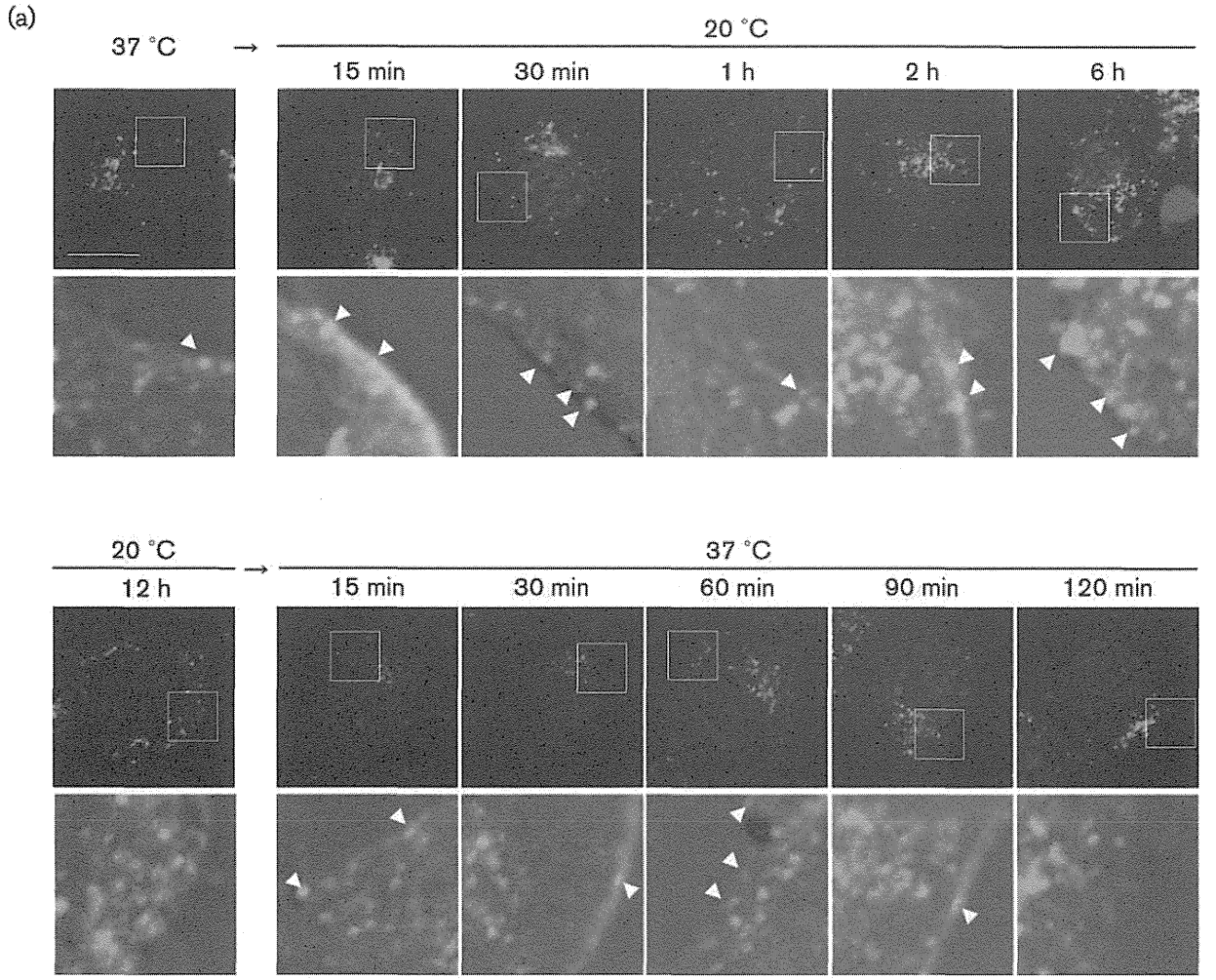
(a)
37 °C
20 °C
15 min
30 min
1 h
2 h
6 h
20 °C
12 h
37 °C
15 min
30 min
60 min
90 min
120 min

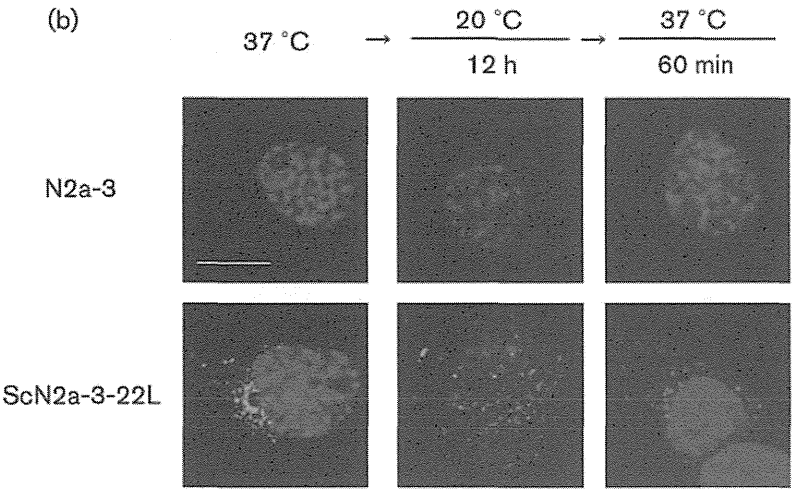
(b)
37 °C
20 °C
12 h
37 °C
60 min
N2a-3
ScN2a-3-22L

Fig. 6. Changes in the localization of PrP^{Sc} during incubation at 20 °C and subsequent incubation at 37 °C. (a) Temperature-dependent localization of PrP^{Sc} in ScN2a-3-22L cells. ScN2a-3-22L cells were grown on a chamber slide at 37 °C. The cells were then incubated at 20 °C for the indicated periods for up to 12 h. After 12 h incubation at 20 °C, the cells were incubated at 37 °C for up to 120 min as indicated. The cells were then fixed and subjected to PrP^{Sc}-specific staining using mAb 132. The upper panels show merged images of PrP^{Sc} (green) and nuclei (blue). The bottom panels show high magnification images of the boxed regions in the corresponding upper panels that were merged with a DIC image. The arrowheads point to representative examples of PrP^{Sc} signals at the cell surface. Bar, 10 μm. (b) Specificity of PrP^{Sc} staining. N2a-3 or ScN2a-3-22L cells cultured on a chamber slide at 37 °C were subsequently incubated at 20 °C for 12 h and then incubated at 37 °C for 60 min. These cells were fixed and subjected to PrP^{Sc}-specific staining using the mAb132. Bar, 10 μm.

labelling is an important factor for PrP^{Sc}-specific detection (Dron *et al.*, 2009). Indeed, this property of the mAb 132 allowed us to perform more precise PrP^{Sc} detection using IFA because the lack of, or trace PrP^{C} signal means that specific manipulation of the threshold setting during data acquisition can be minimized. Since mAb 132 reacts with denatured PrP^{C} and PrP^{Sc} in immunoblotting (Kim *et al.*, 2004b), the reason why mAb 132 cannot detect PrP^{C}, but can detect PrP^{Sc}, in cells pre-treated with GdnSCN remains unclear. However, one possible explanation is that the epitope for mAb 132 on PrP^{C} may not be exposed by the relatively short denaturation period (10 min exposure to GdnSCN). Alternatively, it is possible that once the epitope for mAb 132 on PrP^{C} has been exposed by denaturation with GdnSCN, PrP^{C} may quickly refold into a conformation that prevents access of mAb 132 to the epitope after the removal of GdnSCN. In contrast, PrP^{Sc} was detected in prion-infected cells after denaturation with GdnSCN (Fig. 1), indicating that the epitope-containing region of PrP^{Sc} molecules, unlike that of PrP^{C}, remained antibody-accessible. PrP^{Sc} has been reported to refold into a PrP^{C}-like form after strong denaturation with GdnHCl (Callahan *et al.*, 2001; Kocisko *et al.*, 1996). Given that short-term exposure of GdnSCN will not completely denature PrP^{Sc}, and that PrP^{Sc} exists as an oligomer, intermolecular interaction among neighbouring PrP molecules may disturb the refolding of denatured PrP^{Sc} and as a consequence, the epitope for mAb 132 on PrP^{Sc} molecule may remain accessible to the antibody.

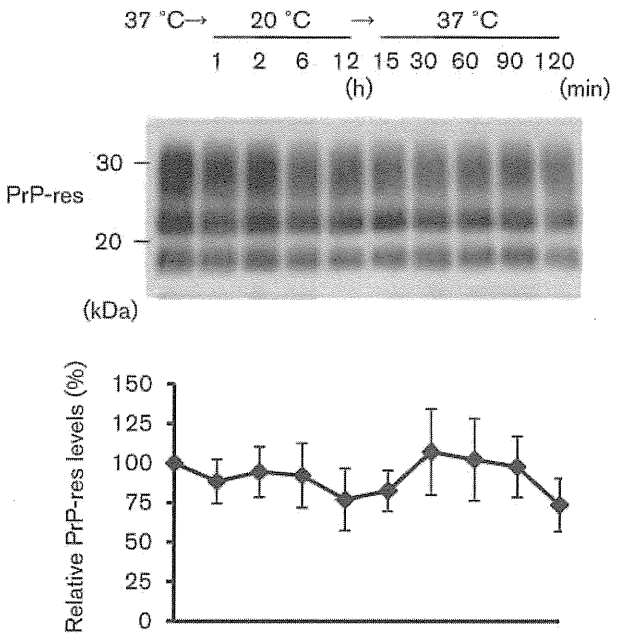

Fig. 7. Amount of PrP-res. ScN2a-3-22L cells cultured on 60 mm dishes at 37 °C were transferred to 20 °C and incubated for 1–12 h. After 12 h of incubation, the cells were incubated again at 37 °C for 15–120 min. The cells were lysed at the indicated time points and were subjected to immunoblotting for PrP-res detection. Sample volume equivalent to 4×10^{5} cells were loaded on each lane. A representative immunoblot image is shown on the top and the graph at the bottom shows the level of PrP-res relative to its level at time 0. The means and SD of four independent experiments are depicted.

In agreement with previous reports (Marijanovic *et al.*, 2009; Pimpinelli *et al.*, 2005; Taraboulos *et al.*, 1990; Veith *et al.*, 2009), we confirmed the widespread intracellular distribution of PrP^{Sc} throughout endocytic compartments in prion-infected cells (Fig. 3). PrP^{Sc} was not only present in early and late endosomes/lysosomes but also in cellular compartments at the peri-nuclear regions, at least some of which are thought to be the ERC, through which exogenously derived Tfn, StxB and CtxB are transported during their intracellular trafficking (Fig. 4). In this study, we observed the extensive co-localization of PrP^{Sc} with flotillin-1 in ScN2a-3-22L cells (Fig. 3). This result is inconsistent with the report by Pimpinelli *et al.* (2005), in which PrP^{Sc} in the Chandler strain-infected N2a cells was not co-localized well with flotillin-1. It remains to be elucidated how differences in prion strains and cell types influence the intracellular distribution of PrP^{Sc}.

Recent immunofluorescent and electron microscopy studies have also proposed the presence of PrP^{Sc} at the ERC (Godsave *et al.*, 2008; Marijanovic *et al.*, 2009). The ERC is a membranous tubular compartment in the vicinity of the nucleus and is defined by the presence of Rab11a and/or Tfn-bound Tfn receptor (Grant & Donaldson, 2009; Murphy *et al.*, 2005). Some internalized plasma membrane proteins such as Tfn receptor, the LDL receptor and GPI-anchored proteins including PrP^{C} are transported from the early endosomes to the ERC and are then sorted to their target sites including the plasma membrane (Magalhães *et al.*, 2002; Mayor & Riezman 2004; Morris *et al.*, 2006;